Journal of Molecular Graphics and Modelling 27 (2008) 546–557

Contents lists available at ScienceDirect

Journal of Molecular Graphics and Modelling

journal homepage: www.elsevier.com/locate/JMGM

Strategies for generating less toxic P-selectin inhibitors: Pharmacophore modeling, virtual screening and counter pharmacophore screening to remove toxic hits

Ravi Shekar Ananthula [a], Muttineni Ravikumar [a,*], A.B. Pramod [a], Kishore Kumar Madala [a], S.K. Mahmood [b,*]

[a] BioCampus, GVKBIO S-1, Phase-1, Technocrats Industrial Estate, Balanagar, Hyderabad, Andhra Pradesh 500037, India
[b] Bioinformatics Division, Environmental Microbial Laboratory Department of Botany, Osmania University, Hyderabad, Andhra Pradesh 500007, India

ARTICLE INFO

Article history:
Received 20 September 2007
Received in revised form 10 September 2008
Accepted 10 September 2008
Available online 20 September 2008

Keywords:
Virtual screening
Pharmacophore
Docking
P-selectin
DHOD

ABSTRACT

This paper describes the generation of ligand-based as well as structure-based models and virtual screening of less toxic P-selectin receptor inhibitors. Ligand-based model, 3D-pharmacophore was generated using 27 quinoline salicylic acid compounds and is used to retrieve the actives of P-selectin. This model contains three hydrogen bond acceptors (HBA), two ring aromatics (RA) and one hydrophobic feature (HY). To remove the toxic hits from the screened molecules, a counter pharmacophore model was generated using inhibitors of dihydrooratate dehydrogenase (DHOD), an important enzyme involved in nucleic acid synthesis, whose inhibition leads to toxic effects. Structure-based models were generated by docking and scoring of inhibitors against P-selectin receptor, to remove the false positives committed by pharmacophore screening. The combination of these ligand-based and structure-based virtual screening models were used to screen a commercial database containing 538,000 compounds.

1. Introduction

Leukocyte emigration from the vasculature into tissue upon inflammatory stimulus, involves a cascade of events. Leukocyte rolling, the initial step, is followed by firm adhesion and activation, trans-endothelial migration, and penetration into tissue [1]. Over the last decade, several studies have collectively suggested that the cell adhesion molecules E- and P-selectin expressed on the endothelium play an important and overlapping roles in the initial leukocyte rolling. In addition, it is clear that leukocyte rolling is an important and feasible target for the prevention and treatment of inflammatory diseases [2], such as rheumatoid arthritis (RA), a systemic immune disorder characterized by articular joint inflammation and destruction [3]. Further more, selectins are well-established therapeutic targets for the prevention and treatment of inflammatory diseases [4–8]. Several recent studies have also demonstrated a key role of selectins in atherosclerosis, with P-selectin playing crucial role in disease [9–12]. Elevated levels of E- and P-selectin have been observed in inflammed joints of RA patients [13]. P-selectin is the predominant selectin in leukocyte recruitment and is expressed on the endothelium minutes after stimulation [13]. The role of P-selectin dependent inflammatory cell migration in adjuvant-induced arthritis (AIA) has also been demonstrated [14]. Numerous studies using knock-out animal models or protein therapeutics have shown that inhibiting the P-selectin glycoprotein ligand 1 (PSGL-1) interaction with P-selectin results in reduced atherosclerotic lesion development [15], reduced myointimal proliferation [16,17], and reduced venous thrombosis [18,19]. Treatment with a P-selectin inhibitor in a chronic fashion, therefore, has potential to prevent and treat atherosclerotic vascular disease. These findings stress the necessity for developing novel and less toxic P-selectin selective inhibitors which could be clinically used as the therapeutics for the inflammatory lesions.

In the past, the pharmaceutical industry has primarily employed the process of high throughput screening (HTS) to identify and optimize new drug like lead-compounds. HTS is an expensive process involving combinatorial chemistry coupled with the experimental screening of large chemical libraries against a relevant therapeutic target. Virtual screening has become an integral part of the drug discovery process in recent years [20] and provides a rational alternative to the traditional HTS. The main goal of a virtual screening is to come up with novel chemical structure

* Corresponding authors. Tel.: +91 9989889075.
E-mail addresses: ravambio@gmail.com (M. Ravikumar), skmahmood@osmania.ac.in (S.K. Mahmood).

1093-3263/$ – see front matter © 2008 Elsevier Inc. All rights reserved.
doi:10.1016/j.jmgm.2008.09.007

hits that yield a unique pharmacological profile. Thus, success of a virtual screening (VS) is defined in terms of finding interesting new scaffolds rather than many hits. Recently, VS has experienced increased attention mainly due to the rise in available datasets and VS techniques created by successful screening studies [21,22]. The use of VS technologies have also aided in the identification of bioactive molecules from natural products [23]. VS methods are often divided into structure-based VS (SBVS) [24,25] and ligand-based VS (LBVS) [26,27]. In the present study we have used the combination of SBVS and LBVS for the screening of new compounds against P-selectin. In LBVS, 3D-pharmacophore and Lipinski's rule of 5 and in SBVS, docking methods were used for the discovery of new compounds.

Some of the active compounds of P-selectin are having toxicity issues due to inhibition of dihydrooratate dehydrogenase (DHOD). The flavin enzyme dihydroorotate dehydrogenase (EC 1.3.99.11) catalyzes the oxidation of dihydroorotate to orotate, the fourth step in the de novo pyrimidine biosynthesis of UMP. The pathways involving DHOD in biosynthesis of UMP are described in reports [28]. The inhibition of DHOD causes a lowering of the intracellular pools of uracil, cytosine, and thymine nucleotides in cells, which makes DHOD attractive drug targets [29]. So, this enzyme is been used as a valid drug target for different clinical therapeutic applications such as cancer and arthritis. Brequinar and atovaquone, which are DHOD inhibitors have shown promising results as antiproliferative, immunosuppressive, and antiparasitic agents [30]. Subsequently, inhibition of DHOD by P-selectin inhibitors may cause toxic effects leading to cell death and immunosuppression.

Few studies have found that the non-selective inhibitors of P-selectin also show inhibitory activity against DHOD [31]. No doubt DHOD is acting as a drug target for arthritis, but it also acts as target for cancers and inhibition of DHOD can cause death of cells. Our aim is to develop selective P-selectin inhibitors which do not having binding towards DHOD so that the inflammatory process can be subsided without causing cell death and to obtain such compounds we tried to generate a novel screening method. So, in our VS method we have generated pharmacophore model of DHOD inhibitors which is used as counter pharmacophore in the virtual screening strategy (Fig. 1) to identify and remove the active hits of DHOD in the database and retrieve only less toxic and P-selectin selective inhibitors.

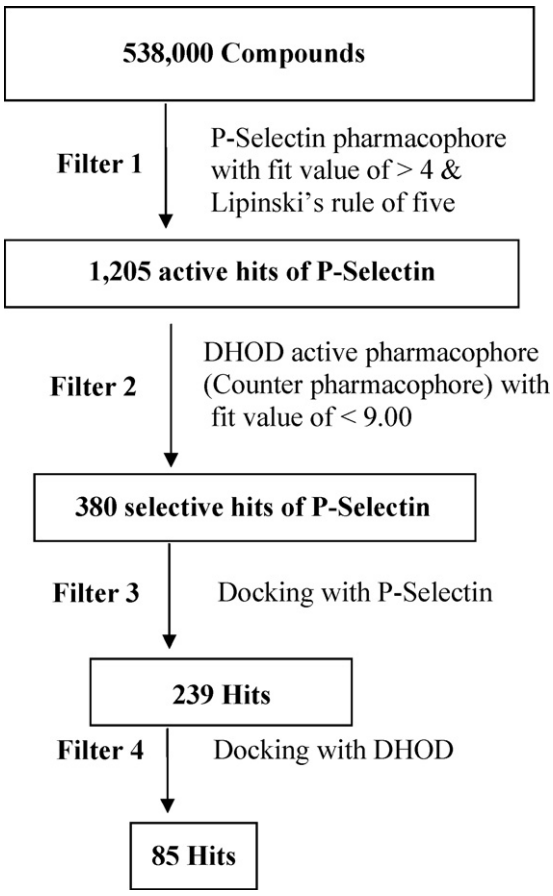

Fig. 1. Virtual screening protocol for discovery of less toxic P-selectin inhibitors.

2. Materials and methods

Biological data: For modeling studies, a data set of molecules having activities against both P-selectin and DHOD were selected from the literature [32,33]. For the generation of P-selectin and DHOD pharmacophores, training sets containing 27 and 17 molecules were selected, respectively (Figs. 2 and 3). These molecules were selected on the basis of structural diversity.

2.1. Molecular modeling

The geometry of each compound was built using the builder module of Cerius2 (Version 4.10) on a silicon graphics Octane2 workstation. All the structures were minimized using the steepest descent algorithm with a convergence gradient value of 0.001 kcal/mol. Partial atomic charges were calculated using the Gasteiger method. Further geometry optimization was carried out for each compound with the MOPAC 6 package (Software) using the semi-empirical AM1 Hamiltonian.

All the molecules were imported into CATALYST (Version 4.10) and conformational models of all molecules for P-selectin and DHOD datasets were generated using the 'best quality' conformational search option within the Catalyst Confirm module using the 'Poling' algorithm [34]. A maximum of 250 conformations were generated for each compound to ensure maximum coverage in the conformational space within an energy threshold of 20.0 kcal/mol above the global energy minimum. Instead of using just the lowest energy conformation of each compound, all conformational models for each molecule in training set were used in catalyst for pharmacophore hypothesis generation. Hence, this search procedure will probably identify the best 3D arrangement of chemical functionalities explaining the activity variations among the training set.

2.2. Pharmacophore modeling

CATALYST includes two separate pharmacophore-modeling modules, namely: HypoGen and HipHop. HypoGen enables automatic pharmacophore construction by using a collection of at least 16 molecules with bioactivities spanning over four orders of magnitude. On the other hand, HipHop generates common feature pharmacophores regardless to the activities of the training compounds. Still, both modules generate 3D pharmacophres that can be used as search queries to virtually screen 3D-structural libraries. However, in the current project, P-selectin inhibitors are having activity in the range of two orders and hence we avoided using HypoGen for generation of pharmacophore, which requires the bioactivity spread of inhibitors to be in four logarithmic cycles. Therefore, we employed HipHop to generate common feature pharmacophore(s) for P-selectin inhibitors.

HipHop identifies 3D spatial arrangements of chemical features that are common to active molecules in a training set. These

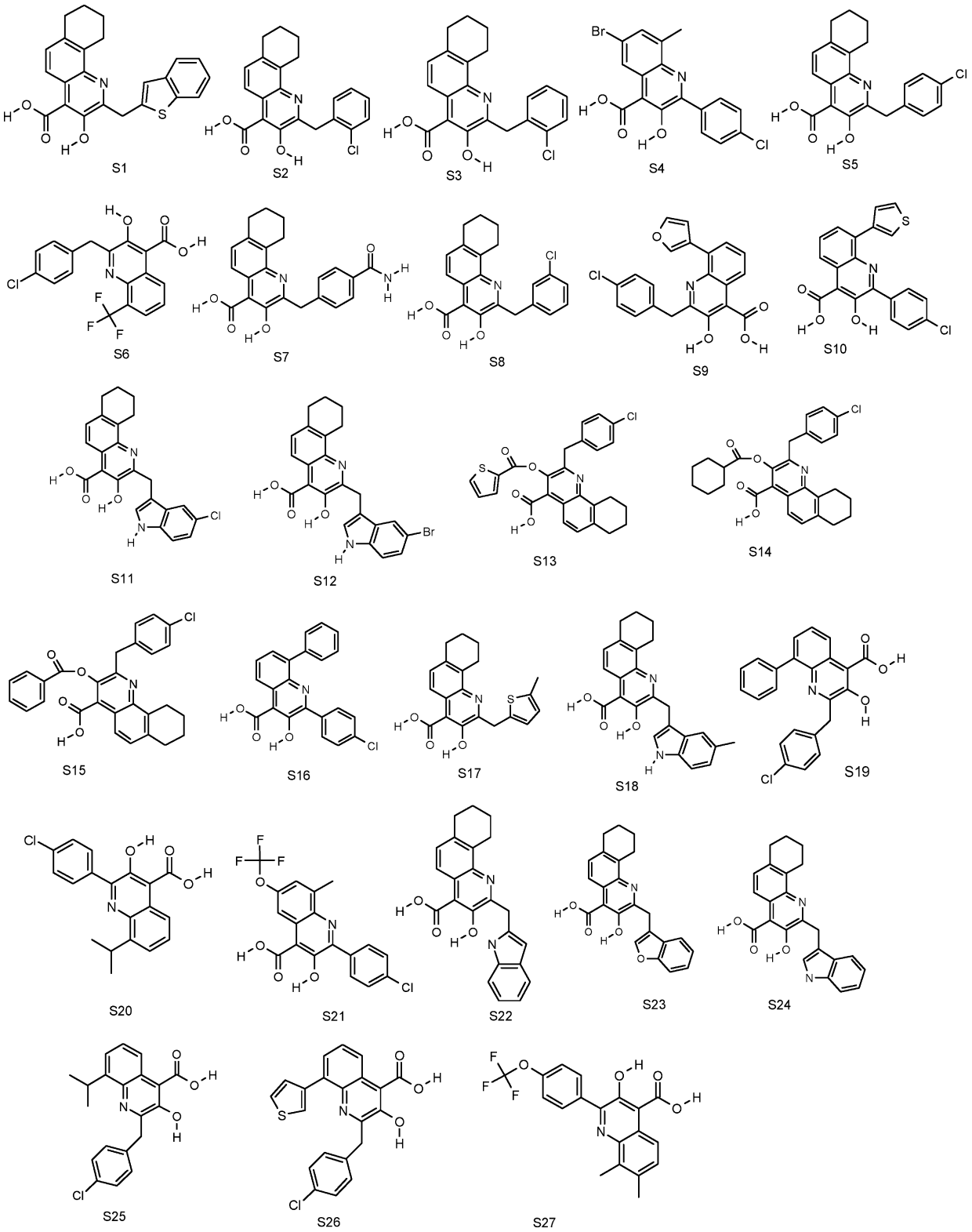

Fig. 2. 2D chemical structures of the 27 molecules forming the training set used to obtain HipHop pharmacophore hypotheses.

configurations are identified by a pruned exhaustive search, starting from small sets of features and extending them until no larger common configuration is found. Active training set members are evaluated on the basis of the types of chemical features they contain, along with the ability to adopt a conformation that allows those features to be superimposed on a particular configuration. The user defines how many molecules must map completely or partially to the hypothesis via the Principal and MaxOmitFeat parameters. These options allow broader and more diverse hypotheses to be generated. The resultant pharmacophores are ranked as they are built. The ranking is a measure of how well the active training molecules map onto the proposed pharmacophores,

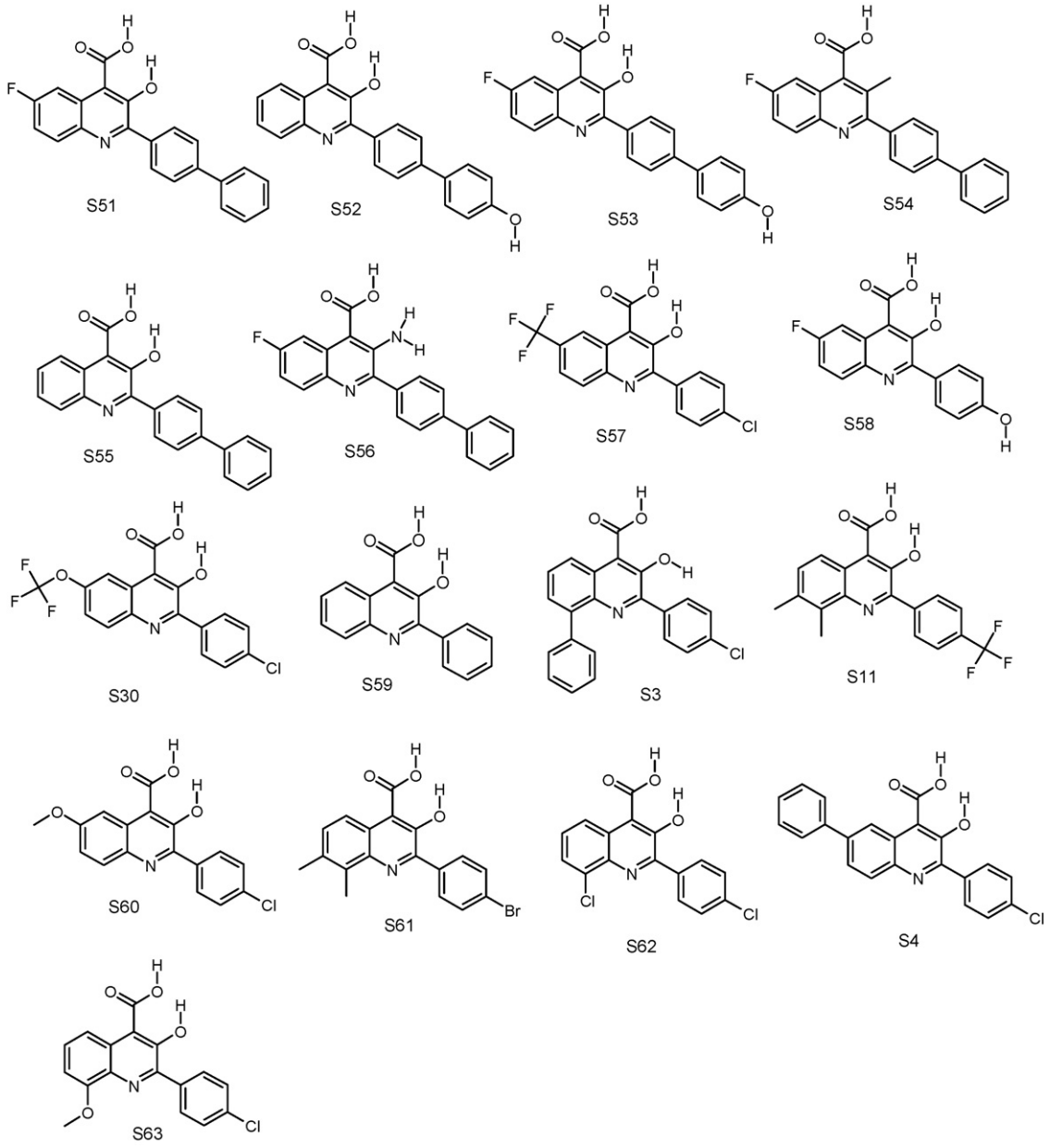

Fig. 3. Training set molecules taken for DHOD pharmacophore (HYPOGEN) generation.

as well as the rarity of the pharmacophore model. If a particular pharmacophore is "rare" then it will be less likely to map to an inactive compound and therefore it will be given a higher rank. HipHop returns by default a maximum of 10 high-ranking pharmacophores from each automatic run. A diverse subset of 27 training compounds was selected for pharmacophore modeling (as shown in Table 1). HipHop was instructed to explore up to six-featured pharmacophoric space for the following possible features: hydrogen bond acceptor (HBA), hydrogen bond donor (HBD), hydrophobic (HY) and ring aromatic (RA). Furthermore, the number of features of any particular type was allowed to vary from 0 to 5. We defined IC50 (or Ki) value ranging from 75 to 275 μM as the activity/moderate activity cutoff. Inhibitors of IC50 (or Ki) values <150 mM were regarded as "actives" and were assigned Principal and MaxOmitFeat values of 2 and 0, respectively, to ensure that all of their chemical features will be considered in building the pharmacophore space. On the other hand, inhibitors of IC50 (or Ki) >150 mM were considered moderate actives and were assigned Principal values of 1.

The activities of DHOD (IC50) are ranging from 0.005 to 310 μM, hence HypoGen was used for the generation of pharmacophore. HypoGen generates the pharmacophore model that explains variations in activity across a set of molecules for the available experimental information such as 2D structures and biological activities of a set of molecules. It generates the model that contains the common features present in the active compounds but not in inactive compounds, and therefore the generated model can be used as a counter pharmacophore to remove active hits of DHOD from the virtual library.

The training set molecules [17] associated with their conformations was submitted to the Catalyst hypothesis generation (HypoGen) (Fig. 3). Features such as hydrogen-bond donor (HBD), hydrophobic (HY), positive ionizable and ring aromatic (RA) were included for the pharmacophore generation on the basis of

Table 1
The training list used for pharmacophore modeling of P-selectin inhibitors.

Comp. S. no.	IC50 (μM)	Principle value	Max omit
S1	75	2	0
S2	100	2	0
S3	123	2	0
S4	125	2	0
S5	125	2	0
S6	125	2	0
S7	125	2	0
S8	138	2	0
S9	150	2	0
S10	175	1	1
S11	175	1	1
S12	175	1	1
S13	175	1	1
S14	175	1	1
S15	190	1	1
S16	200	1	1
S17	200	1	1
S18	200	1	1
S19	200	1	1
S20	225	1	1
S21	225	1	1
S22	225	1	1
S23	225	1	1
S24	225	1	1
S25	225	1	1
S26	225	1	1
S27	240	1	1

common features present in the study molecules. Ten pharmacophore models with significant statistical parameters were generated. The best model was selected on the basis of a highest correlation coefficient (r), lowest total cost and root mean square deviation (rmsd) values (for more details on cost values, see Ref. [30]).

2.3. Docking studies

For our structure-based drug designing studies we utilized X-ray crystal structures of P-selectin and DHOD with PDB Codes, 1G1S and 1D3G, respectively. The two crystal structures (1G1S and 1D3G) are having resolution of 1.90 and 1.60 Å, respectively. Protein was prepared by removal of solvent molecules coupled with the addition of hydrogen atoms, and the structures of protein and ligand were combined in a single macromodel (Schrodinger, Inc.) file. The active site was visually inspected and the appropriate corrections were made for tautomeric states of histidine residues, orientations of hydroxyl groups, and protonation states of basic and acidic residues. The hydrogen atoms were minimized for 3000 steps with macromodel in the MMFF force field [35–37], while constraining all the heavy atoms (non-hydrogen) to their original positions. The protein with optimized hydrogen coordinates was finally saved as a separate file to be used for docking. All the known actives and the database hits were docked into the active site of the target protein using the Glide program, version 3.0 (Schrodinger, Inc.) in standard docking mode (Glide SP) [38,39]. The binding region was defined by a 12 Å_12 Å_12 Å box centered on the centroid of the crystallographic ligand to confine the centroid of the docked ligand. No scaling factors were applied to the van der Waals radii. Default settings were used for all the remaining parameters. The top 20 poses were generated for each ligand. The docking poses were then energy minimized with macromodel using OPLS2001 force field, and docked keeping ligand flexible and receptor rigid. Best pose was selected on the basis of the interactions formed between the ligands and active site amino acids and Glide score.

2.4. Validation of virtual screening model

The validation of virtual screening model is done based on the protocol which initially checked the ability of the common featured P-selectin pharmacophore to pick P-selectin inhibitors in the database. Picked P-selectin inhibitors were further screened to eliminate DHOD specific compounds using HypoGen based DHOD pharmacophore (counter pharmacophore). The resultant molecules were docked with P-selectin to reduce false positives. The final hits were refined by docking them with DHOD to get only those having P-selectin selectivity. For the validation of virtual screening procedure, a database containing 1000 compounds was considered. The database included 160 known actives of P-selectin in which 37 compounds were also having activity against DHOD. In 37 actives of DHOD, only 13 are highly active compounds (IC50 < 1 μM).

2.5. Virtual screening

An in-house database of 538,000 compounds was used in the virtual screening process. The validated P-selectin pharmacophore model was used as a 3D structural query in the virtual screening. The "best flexible search" method in Catalyst is used for the searching of database. The hits obtained were further filtered using Lipinski's rule of five and with the fit score of 4.00. To get selective or less toxic compounds from these hits, DHOD pharmacophore model (counter pharmacophore) was used. To remove false positives from the remained ones, docking was employed on these molecules. For final refining of the molecules for P-selectin selectivity, the hits were docked into the active site of DHOD. The molecules having poor or no interactions with DHOD were considered as less toxic P-selectin selective inhibitors. The scaffold of the hits obtained by such virtual screening methodology is having properties contrasting to that possessed by a privileged scaffold that has affinity to a broader target space, so we named virtual hit scaffold obtained here as "veto" scaffold, which preventing binding to a larger target space.

3. Results and discussion

A structurally diverse training subset was carefully selected from the collected compounds for HipHop modeling (Fig. 2). Effective pharmacophore modeling requires training sets of adequate structural diversity to elucidate the common functional features responsible for ligand–receptor affinity across wide ligand space. Hip-Hop was instructed to explore up to six-featured pharmacophoric geometry. Higher-feature pharmacophores were found to be too restrictive and having limited coverage, i.e. they captured limited number of hits upon using them as 3D search queries. On the other hand, lower-featured pharmacophores are non-selective and tend to capture most (or all) of the inhibitors without effective discrimination against least potent inhibitors. Furthermore, by careful evaluation of the binding pocket and structure of active inhibitors, we realized that six-featured pharmacophores can describe the interactions of the vast majority of active inhibitors within P-selectin binding pocket.

$$\text{fit} = \sum \text{mapped hypothesis features} \times W[1 - \sum \left(\frac{\text{disp}}{\text{tol}}\right)^2 \qquad (1)$$

The software was instructed to explore pharmacophoric models incorporating from zero to five features from any particular selected feature type (i.e. HBA, HBD, HY and RA).

Eventually, 10 optimal pharmacophoric hypotheses were generated. However, they all shared comparable features and

Table 2
The pharmacophoric features of the 10 hypotheses generated by the HipHop automatic run.

Hypothesis	Rank	Features
1	427.432	RRHAAA
2	426.927	RRHAAA
3	426.927	RRHAAA
4	423.757	RRHAAA
5	423.678	RRHAAA
6	422.237	RRHAAA
7	419.651	RRHAAA
8	411.679	RRHAAA
9	378.813	RRHAA
10	373.569	RRHAA

covered properties against a number of 90 compounds. Table 2 shows the pharmacophoric features of the generated models. The highest-ranking model (HipHop l) is comprised of three HBAs, two HBDs and one hydrophobic feature. Fig. 4 shows the arrangement of pharmacophoric features along with the distances between them.

Fig. 5 shows how HipHop l fits to the highly active inhibitor S1. Evidently, from the figure, the two aromatic features are mapped to the two phenyl rings of the most active compound. Three HBAs are perfectly mapped to O of ethoxy group, carbonyl oxygen and electron rich nitrogen of benzeimidazole ring, respectively. The hydrophobic feature is mapped to the methyl of methoxy group present on the phenyl ring.

The counter pharmacophore model was generated using Hypogen module of catalyst with a training set of 17 DHOD inhibitors (Fig. 3). The statistical results of the pharmacophore model are listed in Table 3. Figure 1S shows the three dimensional arrangement of features along with the distances between the features. This pharmacophore model is used to remove the toxic compounds from the database. The pharmacophore model contains four features including: one positive ionizable, one hydrophobic and two ring aromatic features.

3.1. Docking studies

Docking studies were performed for the 50 P-selectin inhibitors to identify the hot spots that are responsible for specific biological recognition. SP model of Glide software was used for the docking

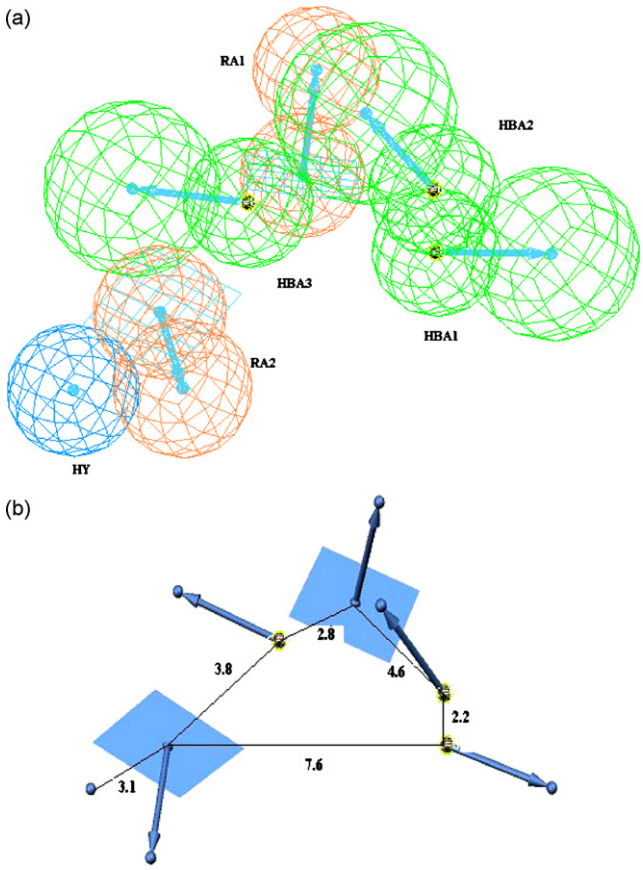

Fig. 4. (a) Top-Ranking HipHop pharmacophore. The hypothesis features are color-coded as follows: ring aromatic (RA), orange; hydrophobic (HY), light blue; hydrogen bond acceptor, green (HBA). (b) Distances (Å) between all features in HipHop.

experiments. All molecules showed the docking score in the range of −9.498 to −5.43 (Table 2S). Fig. 6 shows the binding conformation of the ligand inside the active site of the receptor. As depicted from the figure, hydrogen bond interactions are playing important role in the ligand binding. The carbonyl oxygen of carboxylic group present in the ligand is forming bifurcated hydrogen bond with side chain NH of two amino acids (Lys111 and

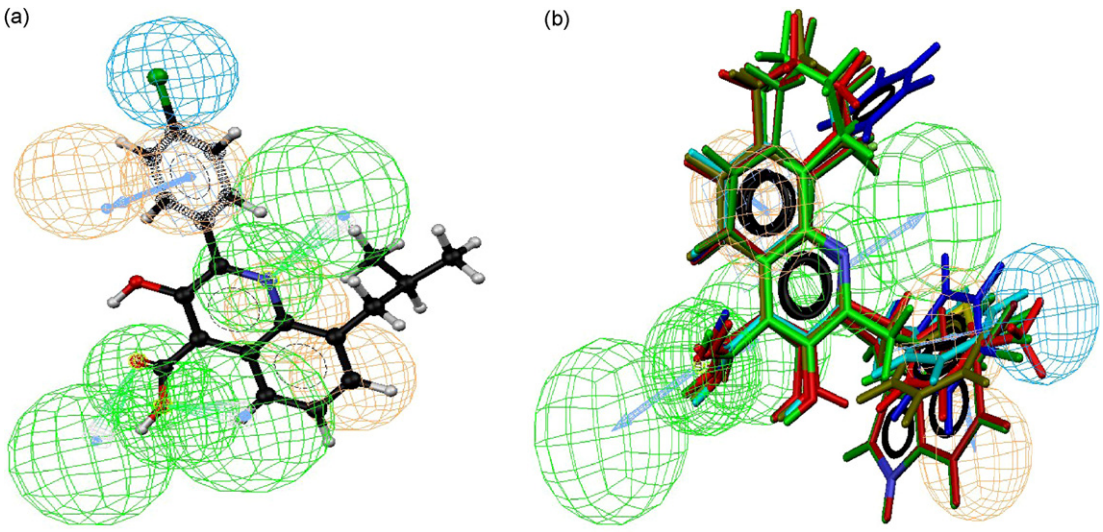

Fig. 5. HipHopl mapped against training P-selectin inhibitors (Table 1): (a) S1 and (b) mapping of the training set molecules to the pharmacophore model.

Table 3
Results of pharmacophore hypothesis generated using training set against DHOD inhibitors.

Hypo no.	Total cost	Cost difference (null-total)	Error cost	RMS	Correlation (r)
1	95.912	−82.728	74.696	1.435	0.929
2	96.524	−82.116	75.495	1.467	0.925
3	96.814	−81.827	75.541	1.469	0.925
4	97.089	−81.551	75.419	1.464	0.926
5	97.089	−81.551	75.620	1.472	0.925
6	97.115	−81.525	76.117	1.492	0.923
7	97.133	−81.507	75.756	1.478	0.924
8	97.135	−81.505	75.896	1.483	0.924
9	97.148	−81.492	75.647	1.473	0.925
10	97.204	−81.436	75.600	1.472	0.925

Arg85) and oxygen of OH in carboxylic group is also forming hydrogen bond interaction with Lys111. These two features also appeared in pharmacophore model (HBA1 and HBA2, Fig. 4). The oxygen atom of OH group present in ligand is forming hydrogen bond interactions side chain NH of Arg85. The electron rich nitrogen of quinoline ring is showing a weak interaction with CH group present in the side chain of Asn84, this feature is represented as HBA3 in the pharmacophore model.

3.2. Validation of VS model

3.2.1. P-selectin pharmacophore model

The HipHop-1 of P-selectin inhibitors was validated for the ability to pick P-selectin actives in a known database. For this validation, the database (D) having 1000 compounds was used, of which 160 (A) were known inhibitors of P-selectin. In 160 known inhibitors, 13 compounds are highly active against DHOD and 24 compounds are moderate to low active against DHOD. This database was screened with HipHop-1, 201 molecules (Ht) were retrieved as hits. Among these hits, 148 (Ha) molecules were known actives. Thus, the enrichment factor (as per Eq. (1)) was found to be 4.60, indicating that it is 4.60 times more probable to pick an active compound from the database than an inactive one. It is retrieving 92.50% of actives from the database; it indicates that pharmacophore model is able to identify the P-selectin active compounds from the database. The major drawbacks of this pharmacophore model are: (i) lack of specificity, i.e. it retrieved entire 13 highly active and 18 moderate to low active compounds of DHOD. (2) It is also retrieving 53 false positives from the database.

$$E = \frac{\mathrm{Ha/Ht}}{A/D} \quad (1)$$

where Ht = the number of hits retrieved, Ha = the number of actives in the hit list, A = the number of active molecules present in the database, and D = the total number of molecules in the database.

3.2.2. DHOD pharmacophore

This model is validated for ability to identify the DHOD actives in the hits of P-selectin retrieved by the respective pharmacophore model. The 201 hits retrieved by P-selectin pharmacophore model were screened with DHOD-pharmacophore model. The model was able to retrieve 12 highly active and 8 moderately active compounds of DHOD, from these 201 compounds. Thus the combination of P-selectin and DHOD pharmacophore models can be used to obtain the P-selectin selective (less toxic) inhibitors from the database.

3.2.3. P-selectin docking model

To remove false positives of P-selectin pharmacophore hits, all the hits were docked into the active site of P-selectin. Out of 53 false positives, 41 compounds showed no interactions or had poor docking score with P-selectin. Thus the combinations of pharmacophore and docking methods have generated less toxic and highly predictable inhibitors of P-selectin.

3.2.4. DHOD docking model

Final conformation of the hits, i.e. whether they are having any interaction with DHOD was done by docking the final hits to the DHOD receptor active site. The final hits obtained after docking to P-selectin were docked into the active site of DHOD and all the

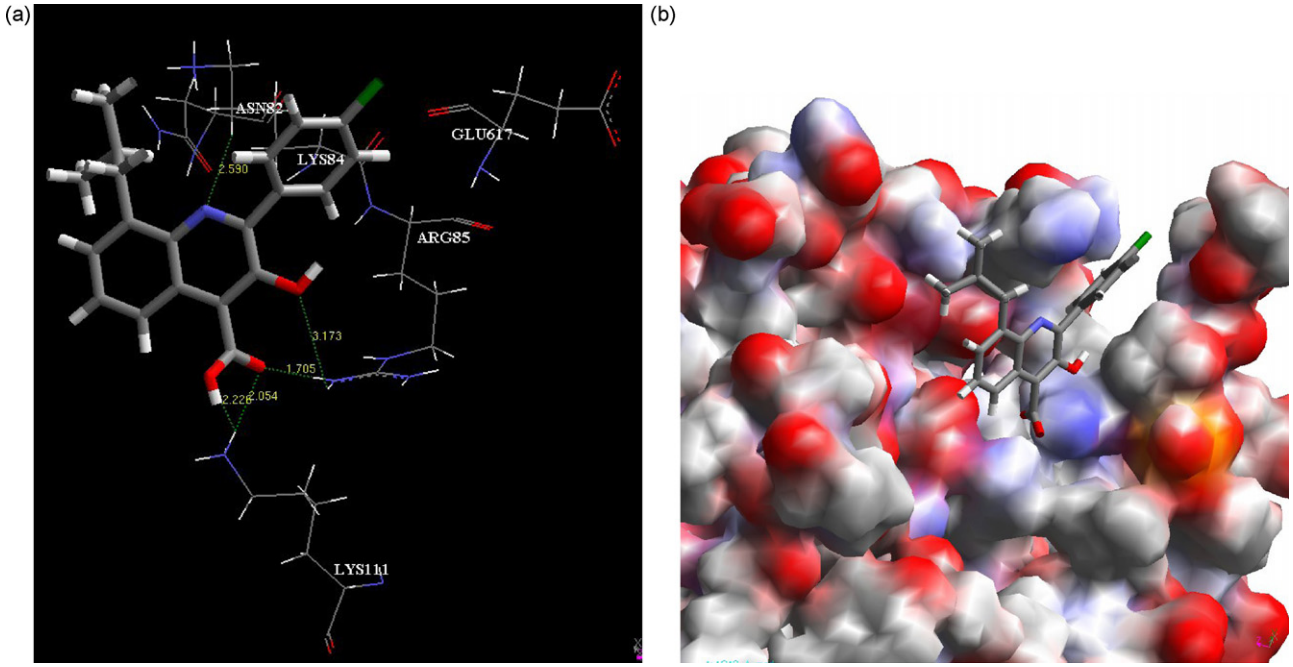

Fig. 6. (a) Docked conformation of the most active compound 1 in the active sites of P-selectin. Broken lines represent hydrogen bonds and (b) Docked pose of compound 1 in P-selectin molecular surface.

Table 4
Examples of best hits obtained from in-house database using HipHop model of P-selectin inhibitors.

Compound number	Mapping of molecule with P-selectin pharmacophore (HipHop model)	Structure	Best fit with P-selectin pharmacophore	Estimated activity with DHOD pharmacophore (μM)
N1	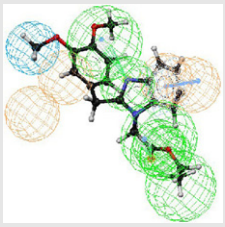	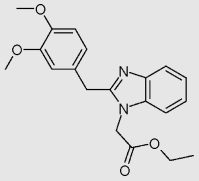	5.798	28
N2	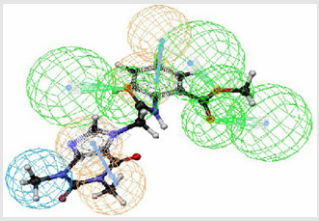	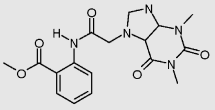	5.659	20
N3	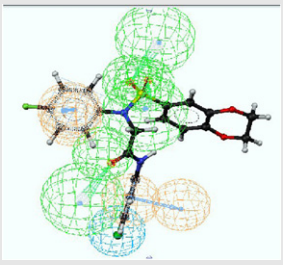	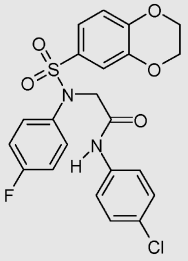	5.624	15
N4	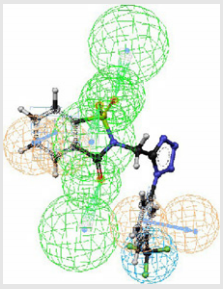	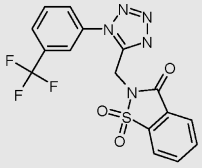	5.614	63
N5	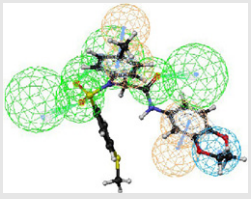	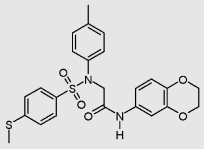	5.559	5
N6	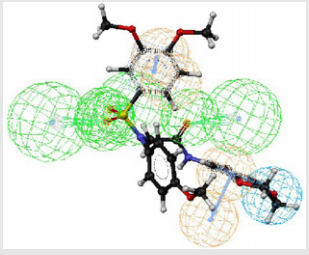	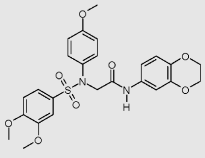	5.553	17

Table 4 (*Continued*)

Compound number	Mapping of molecule with P-selectin pharmacophore (HipHop model)	Structure	Best fit with P-selectin pharmacophore	Estimated activity with DHOD pharmacophore (μM)
N7	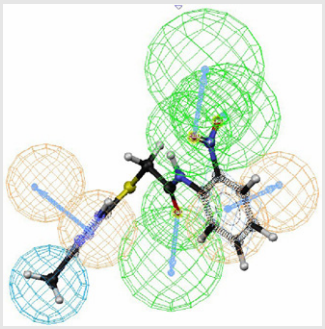	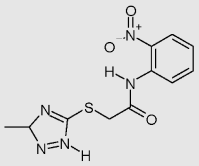	5.546	3
N8	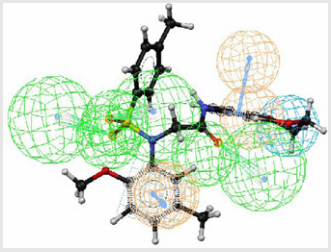	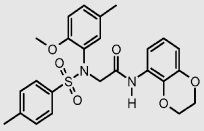	5.546	11
N9	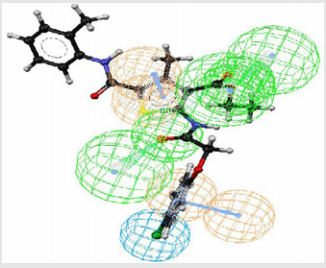	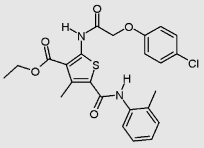	5.497	16
N10	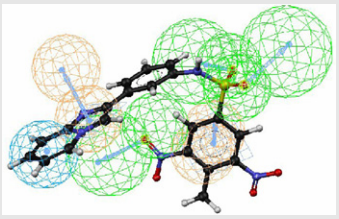	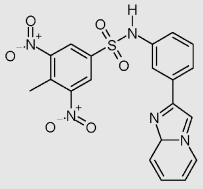	5.497	21
N11	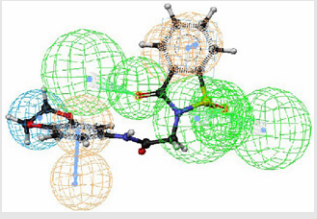	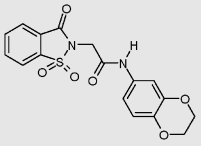	5.486	14

molecules were showing very poor interactions with DHOD receptor.

3.3. Virtual screening of in-house database

The virtual screening protocol is illustrated in Fig. 1. Hypo l was employed as 3D search query to screen the in-house database (538,000 compounds). 6000 molecules were retrieved as Hits. Hits are defined as those compounds that possess chemical groups that spatially overlap (map) with corresponding features within the pharmacophoric model. The hits were subsequently fitted against Hypol (see the fit Eq. (1)), and those having fit values of zero were excluded from subsequent processing. A low fit value indicates that although the chemical functions of the particular hit(s) overlap with the corresponding pharmacophoric features, the centers of the functional groups (of the hit) are displaced from the centers of the corresponding pharmacophoric features, such that the term $P(\text{disp/tol})^2$ in Eq. (1) approaches a value of 1.0 and the overall fit value approaches 0. Therefore, excluding poor fitters to the pharmacophore model improves the success rate of the

retained hits. So, hits with fit value greater than 4.0 were considered for further analysis. The remaining hits (1321 compounds) were filtered according to Lipinski's "rule of five" to retain drug-like molecules. However, we allowed a maximum of one Lipinski's violation to enrich the chemical diversity of the selected hits. This selection retained 1205 hit molecules. To avoid the interactions of these molecules with DHOD receptor, which leads to toxic effects, we have generated pharmacophore model of DHOD receptor and it is used a counter pharmacophore model (1S) to screen the best hits obtained by P-selectin pharmacophore querying of the database. The molecules which showed high fit value (>9.0) with DHOD pharmacophore model were removed and remaining were 380 molecules. In order to eliminate any false positives from these molecules and evaluate the interactions with P-selectin, further docking analysis was carried using Glide. Based on P-selectin binding glide scores, 239 molecules showed high affinity towards the receptor. To confirm the selective affinity of same molecules, they were docked to the DHOD receptor also. Out of 239 molecules 85 molecules were having poor interactions or no interactions with receptor along with supporting low dock scores. Finally these 85 molecules were confirmed as highly selective inhibitors to P-selectin based on screening procedure involving poor fitting to pharmacophore, Lipinski rule violation, fit into counter pharmacophore, P-selectin and DHOD binding.

We are reporting the structures of 10 best molecules of final screen in Table 4. We are in the process of synthesizing the remaining compounds, hence were not disclosing the structures of the compounds. The docking scores of all the 85 compounds are listed in Table 3S. The interactions of the best selective P-selectin molecule with in the active site of P-selection receptor is shown in Fig. 7.

The structure activity relationships of quinoline salicylates against P-selectin observed via docking interactions showed that the oxygen of hydroxyl and carboxyl functionality where having a strong hydrogen bond interactions with Lys111 and Arg85 amino acids (S1 pocket) present in active site of P-selectin (Fig. 8) and thus these groups are essential for activity. These compounds substituted with isopropyl, phenyl, chloro, trifluoromethoxy, trifluoromethyl, and bromo groups at the 8 position are interacting hydrophobically with the S2 hydrophobic pocket (Fig. 8) formed by amino acids (Glu80, Pro81, Asn82 and Lys84) in P-selectin and are showing higher activity. The 3′ and 4′ position substitutions found

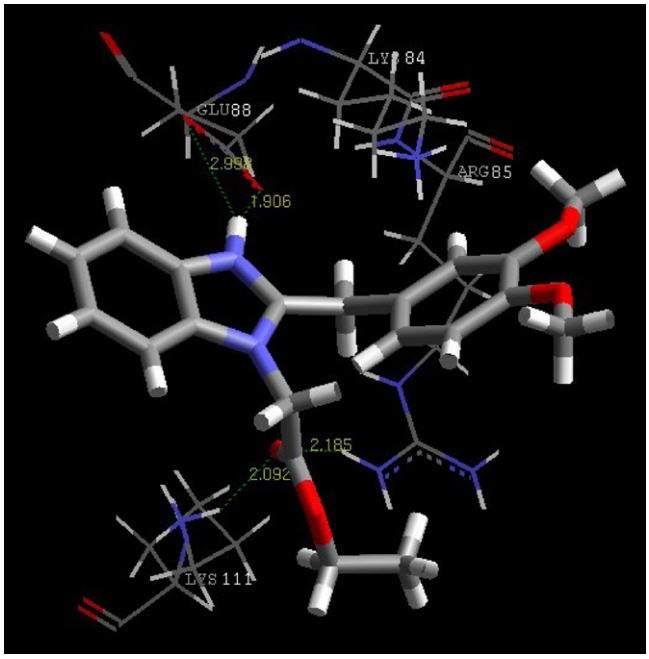

Fig. 7. Interactions of the highest Glide score molecule (VS hit N1) with active site of P-selectin receptor.

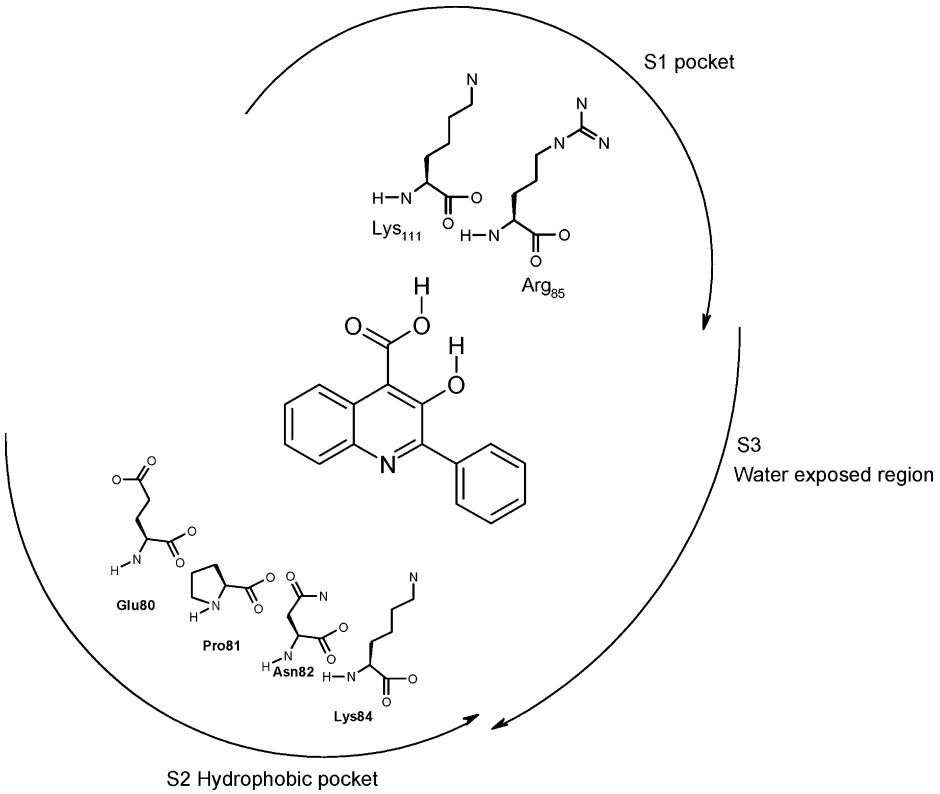

Fig. 8. Schematic representation of ligand interactions with active site amino acids of P-selectin.

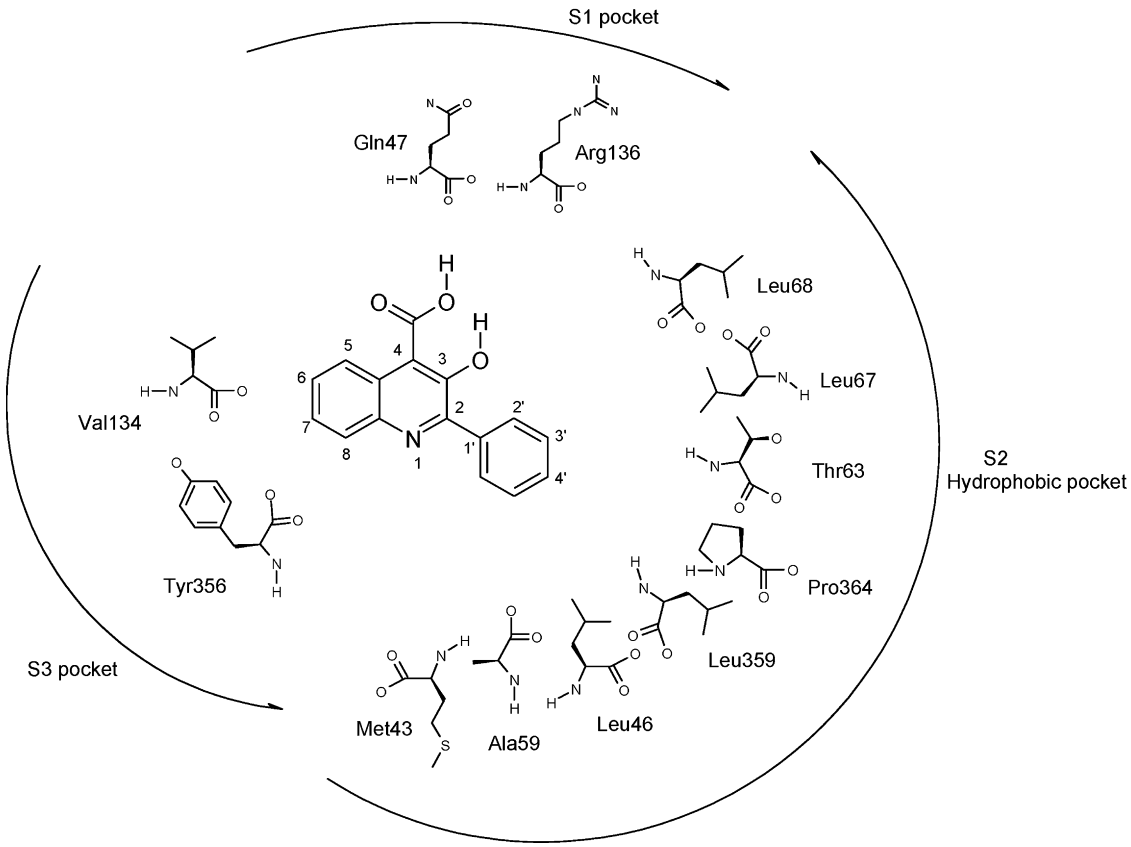

Fig. 9. Schematic representation of ligand interactions with active site amino acids of DHOD.

in C ring are having interactions with the water exposed regions (S3 pocket) of P-selectin (Fig. 8). Small hydrophobic groups at the 4′ position showed good activity.

Docking studies of quinoline salicylates with DHOD revealed that carboxylic group is making interactions with S1 pocket of active site containing Arg136 and Gln47 amino acids (Fig. 9). This indicates that the carboxylic group interactions with the respective amino acids in all of these ligands show at-least some activity against DHOD and do not form a reason for the receptor selectivity for P-selectin. Small hydrophobic groups substituted at 6th position of these salicylates are forming hydrophobic interactions with the Val134 of DHOD and the substitutions at 8th position are showing steric repulsions with Tyr356 (S3 pocket) and hence 6th substituted show higher activity for DHOD. These interactions are useful in designing selective and potent inhibitors of P-selectin by substituting the hydrophobic groups only on 8th position. Moreover the active site of DHOD is having large S2 hydrophobic pocket (Fig. 9) formed by the Met43, Ala59, Leu46, Leu359, Pro364, Thr63, Leu67 and Leu68 at 4th position on the C ring of salicylates but having steric hindrance at 3′ position. Small substitutions at 3′ and 4′ position will show selectivity for P-selection over DHOD.

The 3′ and 4′ position substitutions found in C ring of S1 are having interactions with the water exposed regions of P-selectin. Similar is the situation in the N1 compound, whereas the DHOD crystal ligand the 4th position on the C ring is occupied by the phenyl ring leading to the non-selectivity and decreased activity towards P-selectin.

The compounds which were obtained from the virtual screening protocol are showing the selective interactions with P-selectin amino acids and were showing less or no interactions with DHOD. The best compound of VS (N1), shown in Fig. 7, the benzimidazole is interacting hydrophobically with the S2 hydrophobic pocket formed by amino acids (Glu80, Pro81, Asn82 and Lys84). The carbonyl group of N1 is forming hydrogen bond interactions with Lys111 and Arg85 (S1 pocket, Fig. 8) which is important for activity against P-selectin. The bicyclic rings of ligands is filling the space the potent hydrophobic substitution at the 8th position in S1 is leading to the selectivity for P-selectin affinity. Thus the ‘specialized’ structures obtained in the virtual screening was able to bind only P-selectin as they do not have complimentarily with off-target’s binding site.

4. Conclusions

Drug like molecules having inhibition towards P-selectin receptor were also binding DHOD receptor leading to poor selective binding of molecules and were also showing adverse effects *in vivo*. With an objective to develop a virtual screening method for selecting highly specific P-selectin inhibitors a unique method was used involving P-selection pharmacophore and a counter pharmacophore model (DHOD), strengthened further by docking experiments with both the receptors. This method allowed us to select 85 molecules with high binding affinity towards P-selectin from a database of 538,000 compounds.

Acknowledgement

The authors thank Dr. J.A.R.P. Sarma, Senior Vice-President, GVK Biosciences Pvt. Ltd. for their cooperation and providing software facilities.

Appendix A. Supplementary data

Supplementary data associated with this article can be found, in the online version, at doi:10.1016/j.jmgm.2008.09.007.

References

[1] T.A. Springer, Traffic signals for lymphocyte recirculation and leukocyte emigration: the multistep paradigm, Cell 76 (1994) 301–314.
[2] H. Thorlacius, Selectins as targets in inflammatory diseases, Curr. Med. Chem. Anti-Inflam. Anti-Allergy Agents 3 (2004) 31–38.
[3] (a) R.W. McMurray, Adhesion molecules in auto immune disease, Semin. Arthritis Rheum. 25 (1996) 215–233;
(b) S. Hosaka, M.R. Shah, R.M. Pope, A.E. Koch, Soluble forms of P-selectin and intercellular adhesion molecule-3 in synovial fluids, Clin. Immunol. Immunopathol. 78 (1996) 276–282.
[4] R.P. McEver, R.D. Cummings, Role of PSGL-1 binding to selectins in leukocyte recruitment, J. Clin. Invest. 100 (1997) S97–103.
[5] B. Furie, B.C. Furie, R. Flaumenhaft, A journey with platelet P-selectin: the molecular basis of granule secretion, signaling, and cell adhesion, Thromb. Haemost. 86 (2001) 214–221.
[6] B. Lowe, Glycosylation in the control of selectin counter-receptor structure and function, Immunol. ReV. 186 (2002) 19–36.
[7] D. Vestweber, Regulation of endothelial cell contacts during leukocyte extravasation, Curr. Opin. Cell Biol. 14 (2002) 587–593.
[8] K. Ley, The role of selectins in inflammation and disease, Trends Mol. Med. 9 (2003) 263–268.
[9] B.S. Coller, Leukocytosis and ischemic vascular disease morbidity and mortality: Is it time to intervene? Arterioscler. Thromb. Vasc. Biol. 25 (2005) 658–670.
[10] A.D. Blann, S.K. Nadar, G.Y.H. Lip, The adhesion molecule P-selectin and cardiovascular disease, Eur. Heart J. 24 (2003) 2166–2179.
[11] S.A. Hope, Cellular adhesion molecules and cardiovascular disease. Part II. Their association with conventional and emerging risk factors, acute coronary events and cardiovascular risk, Intern. Med. J. 33 (2003) 450–462.
[12] P. Martins, C. da, N. van den Berk, L.H. Ulfman, L. Koenderman, P.L. Hordijk, J.J. Zwaginga, Platelet-monocyte complexes support monocyte adhesion to endothelium by enhancing secondary tethering and cluster formation., Arterioscler. Thromb. Vasc. Biol. 24 (2004) 193–199.
[13] D.S. Robinson, P.S. Frenette, H. Rayburn, M. Cummiskey, M. Ullman-Cullere, D.D. Wagner, R.O. Hynes, Multiple, targeted deficiencies in selectins reveal a predominant role for P-selectin in leukocyte recruitment, Proc. Natl. Acad. Sci. U.S.A. 96 (1999) 11452–11457.
[14] U.M. Walter, A.C. Issekutz, The role of E- and P-selectin in neutrophil and monocyte migration in adjuvant-induced arthritis in the rat, Eur. J. Immunol. 27 (1997) 1498–1505.
[15] P.C. Burger, D.D. Wagner, Platelet P-selectin facilitates atherosclerotic lesion development, Blood 101 (2003) 2661–2666.
[16] J.G. Bienvenu, J.-F. Tanguay, J.-F. Theoret, A. Kumar, R.G. Schaub, Y. Merhi, Recombinant soluble P-selectin glycoprotein ligand-1-Ig reduces restenosis through inhibition of platelet-neutrophil adhesion after double angioplasty in swine, Circulation 103 (2001) 1128–1134.
[17] S.S. Smyth, E.D. Reis, W. Zhang, J.T. Fallon, R.E. Gordon, B.S. Coller, et al., Beta(3)-integrin-deficient mice but not P-selectin deficient mice develop intimal hyperplasia after vascular injury: correlation with leukocyte recruitment to adherent platelets 1 h after injury, Circulation 103 (2001) 2501–2507.
[18] D. Myers, S. Wrobleski, F. Londy, B. Fex, A. Hawley, R. Schaub, L. Greenfield, T. Wakefield, New and effective treatment of experimentally induced venous thrombosis with anti-inflammatory rPSGL-Ig, Thromb. Haemost. 87 (2002) 374–382.
[19] M.J. Eppihimer, R.G. Schaub, P-selectin-dependent inhibition of thrombosis during venous stasis, Arterioscler. Thromb. Vasc. Biol. 20 (2000) 2483–2488.
[20] M. Stahl, et al., Integrating molecular design resources within modern drug discovery research: the Roche experience, Drug Discov. Today 11 (2006) 326–333.
[21] B.S. Edwards, et al., Integration of virtual screening with high throughput flow cytometry to identify novel small molecule formylpeptide receptor antagonists, Mol. Pharmacol. 68 (2005) 1301–1310.
[22] D.C. Fara, et al. Integration of virtual and physical screening, this issue.
[23] J.M. Rollinger, et al., Strategies for efficient lead structure discovery from natural products, Curr. Med. Chem. 13 (2006) 1491–1507.
[24] A. Good, Structure-based virtual screening protocols, Curr. Opin. Drug Discov. Dev. 4 (2001) 301–307.
[25] P.D. Lyne, Structure-based virtual screening: an overview, Drug Discov. Today 7 (2002) 1047–1055.
[26] T.I. Oprea, H. Matter, Integrating virtual screening in lead discovery, Curr. Opin. Chem. Biol. 8 (2004) 349–358.
[27] P. Willet, Similarity-based virtual screening using 2D fingerprints, Drug Discov. Today 11 (2006) 1046–1053.
[28] http://web.virginia.edu/Heidi/chapter27/chp27.htm#f17.
[29] L.D. Fairbanks, M. Bofill, K. Ruckemann, H.A. Simmonds, Importance of ribonucleotide availability to proliferating T-lymphocytes from healthy humans–disproportionate expansion of pyrimidine pools and contrasting effects of de-novo synthesis inhibitors, J. Biol. Chem. 270 (1995) 29682–29689.
[30] S.P. Liu, E.A. Neidhardt, T.H. Grossman, T. Ocain, J. Clardy, Structures of human dihydroorotate dehydrogenase in complex with anti-proliferative agents, Struct. Fold. Des. 8 (2000) 25–33.
[31] C. Pally, D. Smith, B. Jaffee, R. Magolda, H. Zehender, B. Dorobek, P. Donatsch, C. Papageorgiou, H.-J. Schuurman, Side effects of brequinar and brequinar analogues, in combination with cyclosporine, in the rat, Toxicology 127 (1998) 207–222.
[32] Kaila Neelu, et al., Synthesis and biological evaluation of quinoline salicylic acids as P-selectin antagonists, J. Med. Chem. 50 (2007) 21–39.
[33] Kaila Neelu, et al., 2-(4-Chlorobenzyl)-3-hydroxy-7,8,9,10-tetrahydrobenzo[H]-quinoline-4-carboxylic acid (PSI-697): identification of a clinical candidate from the quinoline salicylic acid series of P-selectin antagonists, J. Med. Chem. 50 (2007) 40–64.
[34] A. Smellie, S.L. Teig, P. Towbin, J. Comput. Chem. 16 (1995) 171.
[35] T.A. Halgren, Merck molecular force field. I. Basis, form, scope, parameterization, and performance of MMFF94, J. Comput. Chem. 17 (1996) 490–519.
[36] T.A. Halgren, Merck molecular force field. II. MMFF94 van der Waals and electrostatic parameters for intermolecular interactions, J. Comput. Chem. 17 (1996) 520.
[37] T.A. Halgren, Merck molecular force field. III. Molecular geometries and vibrational frequencies for MMFF94, J. Comput. Chem. 17 (1996) 553.
[38] R.A. Friesner, J.L. Banks, R.B. Murphy, T.A. Halgren, J.J. Klicic, D.T. Mainz, M.P. Repasky, E.H. Knoll, M. Shelley, J.K. Perry, D.E. Shaw, P. Francis, P.S. Shenkin, Glide: a new approach for rapid, accurate docking and scoring. 1. Method and assessment of docking accuracy, J. Med. Chem. 47 (7) (2004) 1739.
[39] T.A. Halgren, R.B. Murphy, R.A. Friesner, H.S. Beard, L.L. Frye, W.T. Pollard, J.L. Banks, Glide: a new approach for rapid, accurate docking and scoring. 2. Enrichment factors in database screening, J. Med. Chem. 47 (7) (2004) 1750.